Nuclear Mathematical and Computational Sciences: A Century in Review, A Century Anew
Gatlinburg, Tennessee, April 6-11, 2003, on CD-ROM, American Nuclear Society, LaGrange Park, IL (2003)

SOME NEW OBSERVATIONS ON USING A FLUX-LIMITED DIFFUSION THEORY IN TRANSPORT CALCULATIONS

Chukai Yin and Bingjing Su*
University of Cincinnati
Department of Mechanical, Industrial and Nuclear Engineering
Cincinnati, OH 45221-0072, USA
yinc@email.uc.edu; bingjing.su@uc.edu

ABSTRACT

A flux-limited diffusion (called DM thereafter) theory was developed from the Minerbo's maximum entropy Eddington factor as a low-order approximation to transport theory. The DM method has been applied to both time-dependent and steady-state transport problems. Overall, DM was demonstrated to perform reasonably well in solving those radiative transfer and neutron transport problems for which the classic diffusion theory doesn't work. However, two weaknesses were observed in recent numerical tests of the method. One is that for time-dependent radiation penetration problems the flux at the boundary with incident particles, which by physics should increases all the times until reaching equilibrium, may decrease sometimes at very early stage of the transient if very small temporal and spatial mesh sizes are used. The other is that its boundary condition produces ambiguity in the solution at a vacuum boundary which is too sensitive to mesh size. Such numerical behaviors were also observed in the Levermore-Pomraning flux-limited diffusion method. This paper discusses these observations and their numerical causes.

Key Words: flux-limited diffusion, maximum entropy Eddington factor, transport calculation

1. INTRODUCTION

Various variable Eddington factor (VEF) methods were proposed [1-3] as expedient approximate solution techniques for radiative transfer and particle transport problems. Basically, these methods involve solving two moment equations, coupled with a nonlinear closure for Eddington factor. Among all the proposed VEF closures, the Minerbo's maximum entropy Eddington factor [1] is considered superior to others because it was developed in a non-*ad hoc* manner in general geometry by a statistical consideration and was actually verified [4,5] to be correct more often than other closures. Therefore, lots of efforts have been made to apply the Minerbo Eddington factor method in transport computations, especially in the radiative transfer and astrophysics communities. However, there is a numerical obstacle to its applications. Since the Minerbo Eddington factor is a nonlinear function of particle flux, a common practice for solving the VEF equations is to implicitly discretize the moment equations in temporal variable (for time-dependent problems) and then solve the resulting equations by iterating (or updating) the Eddington factor. Such a numerical scheme, no matter how to handle the spatial discretization, may lead to anomalous solutions for some transport problems [6,7]. The numerical stability for this implicit scheme was analyzed [5,6,8]. Specifically it was found that this common implicit

* Corresponding author. Tel. +1 513 556 2960; fax: +1 513 556 3390

scheme leads to stable numerical solutions only for problems that don't involve strong anisotropy in angular flux so that the Eddington factor is always less than 0.556.

To apply the Minerbo's Eddington factor method to a general problem, one can use an explicit upwind scheme such as Riemann solvers to treat the VEF equations [9,10]. Riemann solvers use the explicit scheme to discretize the temporal variable so that the solution at any spatial point is estimated directly from the previous time step's results. In this way, it avoids solving the coupled equations, which is troublesome and may yield anomalous solutions under certain conditions, so that regular solutions are always obtained. This approach has been successfully demonstrated in some recent work [5,9,10]. However, compared to an implicit scheme, such explicit scheme usually has certain disadvantages, as discussed in Ref. [11].

Another way of applying the Minerbo Eddington factor in transport calculations is to derive a nonlinear flux-limited diffusion equation from the VEF moment equations, according to the unified framework for relating flux limiters and Eddington factors developed by Levermore [3]. The details of this derivation were given in Refs. [3] and [5]. The analysis [5] shows that the resulting flux-limited diffusion (called DM thereafter) equation is numerically stable and can be solved by both implicit and explicit schemes. The DM method has been demonstrated for both time-dependent and steady-state transport problems [5,11,12]. Overall, for problems that the classic diffusion theory performs well, DM predicts very close results as the classic diffusion does; however, for problems that the classic diffusion theory doesn't work, DM still performs reasonably well. So the DM method could be useful for solving those problems that transport theory is too expensive to use but the diffusion theory is not adequate.

In recent tests of the method, however, two (additional) weaknesses were observed. One is that for a time-dependent non-equilibrium radiation penetration problem the flux at the incident boundary, which by physics should increase all the times until reaching an asymptote, was found decreasing sometimes during the very early stage of the transient, if very small temporal and spatial mesh sizes are used. The other one is concerned about a vacuum boundary condition developed recently: it demonstrates non-convergence of the flux with mesh sizes at the vacuum boundary; i.e., the solution at a vacuum boundary is too sensitive to mesh size. Such numerical behaviors were also observed in the Levermore-Pomraning (LP) flux-limited diffusion method. We present these numerical behaviors and discuss their causes in this paper. Specifically, we introduce the DM method in the next section for completeness and discuss the two observations in Sec. 3 and Sec. 4, respectively. The last section contains a few concluding remarks.

2. THE DM FLUX-LIMITED DIFFUSION METHOD

Consider the transport equation given by

$$\frac{1}{v}\frac{\partial \psi}{\partial t} + \mathbf{\Omega}\cdot\nabla\psi + \sigma\psi = \int_{4\pi} \sigma_s(\mathbf{\Omega}\cdot\mathbf{\Omega}')\psi(\mathbf{\Omega}')d\mathbf{\Omega}' + \frac{S}{4\pi}, \tag{1}$$

where $\psi(\mathbf{r},\mathbf{\Omega},t)$ is the angular flux; $\mathbf{r}$, $\mathbf{\Omega}$, and t are the spatial, angular, and temporal variables; σ and σ_s are the total cross section and the differential scattering cross section; v is the speed of particles; and $S(\mathbf{r},t)$ is an isotropic source that could be coupled with other equations, such as in the case of non-equilibrium radiative transfer. This transport equation may be considered as

either a gray equation or one of the multi-group transport equations with energy group index omitted. For Eq. (1), the flux-limited diffusion equation derived from the Minerbo VEF description is in the same format as the classic diffusion equation, i.e.,

$$\frac{1}{v}\frac{\partial \phi}{\partial t} - \nabla \cdot D\nabla\phi + \sigma_a \phi = S\,, \tag{2}$$

where $\phi = \int_{4\pi} \psi(\mathbf{\Omega}) d\mathbf{\Omega}$ is the scalar flux. However, the diffusion coefficient D is defined by

$$D = \frac{\lambda_M(R)}{\sigma_{eff}}\,, \tag{3}$$

where the effective cross section σ_{eff} is defined by

$$\sigma_{eff} = \sigma_s(1-\bar{\mu}) + S/\phi \tag{4}$$

with $\bar{\mu}$ being the mean of the cosine of scattering angle. The flux-limiter $\lambda_M(R)$ in Eq. (3) is related to a parameter *R*, defined as

$$R = \left| -\frac{\nabla\phi}{\sigma_{eff}\phi} \right| \tag{5}$$

by a transcendental equation via a parameter *Z*:

$$\lambda_M(R) = 1 - \coth^2 Z + 1/Z^2, \tag{6}$$

$$R = \frac{\coth Z - 1/Z}{1 - \coth^2 Z + 1/Z^2}. \tag{7}$$

For convenience to use in calculations, this relation can be very accurately approximated by

$$\lambda_M \approx \frac{1}{3} - \frac{R^2}{15 - 6.248R^{0.5385} + 9R + 3R^2}\,. \tag{8}$$

The maximum relative error of this approximation is about 0.4% in the whole range of $0 \le R < \infty$.

The specification of a reflective boundary condition is the same for this equation as the classic diffusion equation. For vacuum and incident boundaries, a generalized Marshak boundary condition, due to its simplicity, was developed as [11,12]

$$F_{inc} = \frac{1}{2}\left(\beta\phi + D\nabla\phi \cdot \mathbf{n}\right), \tag{9}$$

where F_{inc} is the incident current at the boundary, i.e.,

$$F_{inc} = \int_{\mathbf{n}\cdot\mathbf{\Omega}<0} (-\mathbf{n}\cdot\mathbf{\Omega})\psi(\mathbf{\Omega}) d\mathbf{\Omega}\,, \tag{10}$$

and $\mathbf{n}$ is the outward unit vector at the boundary. The β in the equation is defined by

$$\beta = 1 + \frac{1-\cosh Z}{Z\sinh Z}, \tag{11}$$

where the parameter *Z* is still related with *R* by Eq. (7). Again for convenience, a rational approximation for β was developed as

$$\beta = \frac{1}{2} + \frac{R^2}{24 - 2.714\sqrt{R} + 7.343R + 4R^{1.5} + 2R^2}\,, \tag{12}$$

with the maximum relative error of 0.8% for $0 \le R < \infty$. Note that in the diffusive limit $R \to 0$, Eq. (11) or (12) yields $\beta = 1/2$, which reduces Eq. (9) to the conventional Marshak boundary condition; and in the streaming limit $R \to \infty$ Eq. (11) or (12) yields the correct value of $\beta = 1$.

Another quite popular flux-limited diffusion theory introduced by Pomraning and Levermore [2] has the same formulation as DM, and its only difference is that the LP flux-limiter λ_{LP} relates with the parameter *R* by

$$\lambda_{LP}(R) = \frac{1}{R}\left[\coth R - \frac{1}{R}\right]. \tag{13}$$

The specification of the boundary conditions for the LP flux-limited diffusion equation is slightly different. For details, readers please refer to Ref. [13].

3. UNPHYSICAL BEHAVIOR AT VERY EARLY TIMES

We consider a time-dependent radiative transfer problem describing radiation penetration into an initially cold homogeneous, purely absorbing, slab of thickness *L*. The radiation is driven by a constant, isotropic intensity incident on the left side of the slab for $t > 0$, with a vacuum boundary on the right side of the slab. The transport equation for radiation intensity $I(x,\mu,t)$, boundary and initial conditions are given by

$$\frac{1}{c}\frac{\partial I}{\partial t} + \mu\frac{\partial I}{\partial x} + \sigma I = \frac{c}{2}\sigma_a B\,, \tag{14}$$

$$I(0,\ \mu,\ t > 0) = 2,\ \ \mu > 0, \tag{15}$$

$$I(L,\ \mu,\ \ t > 0) = 0,\ \ \mu < 0\,, \tag{16}$$

$$I(x,\mu,0) = B(0) = 0\,. \tag{17}$$

The quantity $B(t)$ in the equation is the blackbody energy density, defined as

$$B = aT^4\,, \tag{18}$$

where *a* is the radiation constant and T denotes the material temperature. With the heat conduction and fluid motion neglected, the simple material energy balance equation is given by

$$c_v\frac{\partial T}{\partial t} = c\sigma_a(E - B)\,, \tag{19}$$

where c_v is the material heat capacity and $E(x,\ t)$ is the radiation energy, defined by

$$E(x,t) = \frac{1}{c}\int_{-1}^{1} I(x,\mu,t)d\mu\,. \tag{20}$$

A modified material heat capacity $\gamma = c_v / (4aT^3)$ is introduced [13] to rewrite Eq. (19) as

$$\gamma\frac{\partial B}{\partial t} = c\sigma_a(E - B)\,. \tag{21}$$

We further assume the cross section $\sigma = \sigma_a$ and the modified heat capacity γ being constant in space and independent of the material temperature *T*. Specifically, we take $\gamma = 1$. In addition, *x* is expressed in the unit of $1/\sigma$, *t* in the unit of $1/c\sigma$, and *B* and *E* in the unit of $1/c$. Therefore, the radiative transfer and the material balance equations are finally given by,

$$\frac{\partial I}{\partial t}+\mu\frac{\partial I}{\partial x}+I=\frac{B}{2}, \tag{22}$$

$$\frac{\partial B}{\partial t}=(E-B). \tag{23}$$

The flux-limited diffusion equation corresponding to Eq. (22) is given by

$$\frac{\partial E}{\partial t}-\frac{\partial}{\partial x}(D\frac{\partial E}{\partial x})+E=B \tag{24}$$

where the diffusion coefficient D is defined in Sec. 2, with the replacement of S and ϕ by B and E, respectively. The initial conditions of this equation are

$$E(x,\,0)=B(x,\,0)=0. \tag{25}$$

And the boundary conditions are,

$$F_{inc,L}=1=\frac{1}{2}[\beta E-D\frac{\partial E}{\partial x}],\ \text{at}\ x=0 \tag{26}$$

$$F_{inc,R}=0=\frac{1}{2}[\beta E+D\frac{\partial E}{\partial x}],\ \text{at}\ x=L. \tag{27}$$

When solving the equations, we use fine temporal and spatial meshes ($\Delta t = 10^{-3}$ and $\Delta x = 10^{-4}$), in order to demonstrate the overall performances of different methods. For the flux-limited diffusion methods, we begin with $\lambda=1/3$ and $\beta=1/2$ at $t = 0$ to solve Eqs. (24) – (27). After the solution E is obtained, the values of D and β are updated for the next time step. Since a small time step is used, no internal iteration on these values is performed (because internal iteration has almost no effect on the solution).

Figure 1 compares the transport solution (S_{32}), the DM method (D_M), classic diffusion theory (P_1), and the Levermore-Pomraning flux-limited diffusion method (D_{LP}) solutions for radiation energy $E(x,t)$ at several time steps. We see that the D_M and D_{LP} methods work well: especially at small times, D_M and D_{LP} work much better than P_1. Particularly, D_M and D_{LP} predict a much better transport speed than P_1 so their solutions at the wave-fronts match the transport solutions much better. The solutions for the material energy $B(x,t)$, which is not presented here, show the same conclusion.

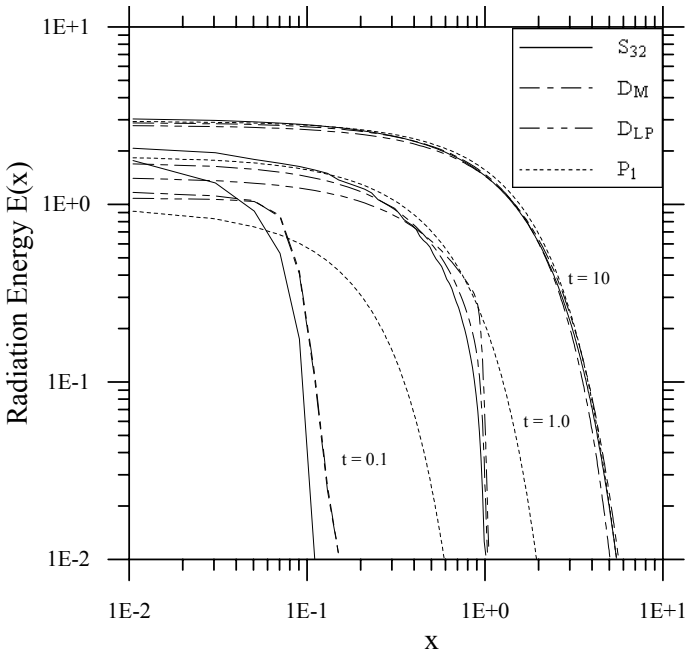

Figure 1. Comparison of Different Solutions

However, careful examination of the flux-limited diffusion solutions at very early times ($t < 0.1$) reveals an unphysical behavior for radiation energy E. Figure 2 plots the solutions

of $E(x,t)$ changing with time at the left boundary $x = 0$. While showing that the flux-limited solutions quantitatively follow the transport solution better than the P_1 solution, it also shows that the flux-limited diffusion solutions don't increase with time smoothly at early times ($t < 0.1$). To see it better, we plot the changing rate of the solution, dE/dt, at $x = 0$ in Figure 3. This figure clearly shows that both the D_M and D_{LP} solutions for dE/dt at $x = 0$ oscillate around zero during the very early stage of the transient so that E actually decreases at some time steps, although that is not so obviously shown in Fig. 2. By physics, the radiation energy at the boundary should increase all the time until reaching equilibrium for this problem. Hence, both the D_M and D_{LP} methods exhibit an unphysical behavior near the boundary at early times.

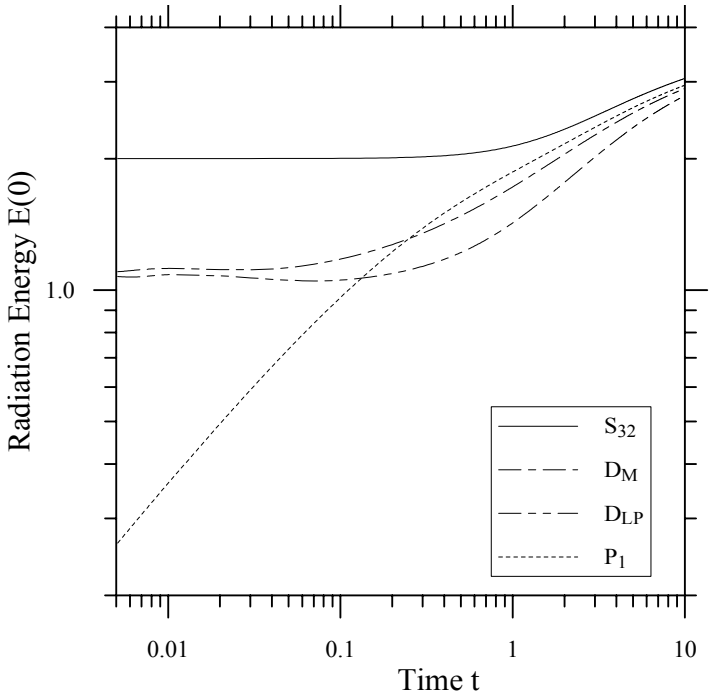

Figure 2. Radiation Energy at the Boundary x = 0

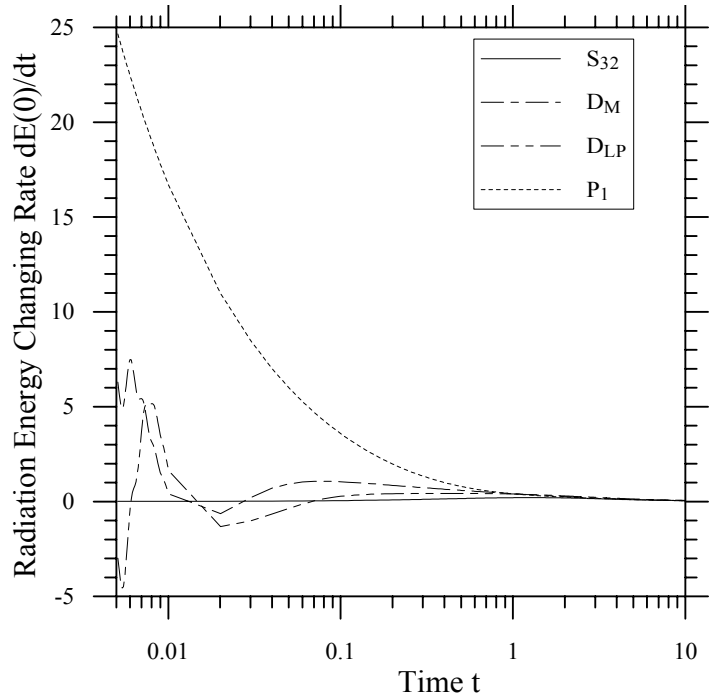

Figure 3. Changing Rate of E(x,t) at x = 0

This behavior definitely is not caused by the coupling with the material energy balance equation, because: (1) At early times, material energy B is negligibly small if compared with radiation energy E; (2) For the same problem, material energy B always increases smoothly with time, even at very early times; and (3) We solved the problem again with the assumption of the radiation field and material energy field in equilibrium (i.e., $B = E$), which reduces the problem to a time-dependent problem only for radiation intensity. However, the D_M and D_{LP} solutions still demonstrate the same unphysical behavior as shown in Figs. 2 and 3.

This unphysical behavior seems to be attributed to the calculation of the diffusion coefficient. By definition (see Sec. 2), the diffusion coefficient in the flux-limited diffusion is a function of scalar flux and its spatial derivative, in addition to material property. For the problem under consideration, the shape of the flux distribution in space changes significantly during early times. Thus, the diffusion coefficient D changes significantly in space, especially near the boundary at early times. If $\partial D / \partial x$ is positive at some point, the gradient of radiation current, which is estimated by $-\partial[D\partial E / \partial x] / \partial x$ in the flux-limited diffusion, could be predicted as positive too, although by physics it should always be negative for this problem. Obviously when $-\partial[D\partial E / \partial x] / \partial x$ is positive, $\partial E / \partial t$ becomes negative at early times because at early times the positive source term B on the right hand side of Eq. (24) is negligible.

We believe the unphysical behavior near the incident boundary is caused by the nonlinear dependence of D on radiation flux. The update on the boundary condition parameter β has no connection with this phenomenon. Numerical tests show that the phenomenon always occurs for this problem as long as the diffusion coefficient D is updated, no matter whether β is updated or kept as a constant in the calculation. In addition, iterating D and β within a time step doesn't cure the behavior either. Furthermore, as discussed in the next section, there are different ways to determine the values of D and β at the boundary; however, those different treatments only quantitatively change the value of $\partial E / \partial t$ near the boundary slightly and qualitatively they all demonstrate the same behavior. Finally, we comment that this behavior is affected by the temporal and spatial meshes used in the calculation. The results represented above are calculated using $\Delta t = 10^{-3}$ and $\Delta x = 10^{-4}$. When $\Delta t = \Delta x = 10^{-4}$ is used, it is found that the oscillation in $\partial E / \partial t$ at the boundary appears sooner in time with larger amplitude. On the contrary, using a larger temporal and spatial mesh size alleviates this oscillation. In fact, when $\Delta t = \Delta x = 10^{-2}$ is used, $\partial E / \partial t$ is found always positive at $x = 0$.

Please note that in spite of this unphysical behavior at very early times, the D_M method overall works well and is still a good approximation for this type of problems.

4. VACUUM BOUNDARY CONDITION

Another strange behavior observed in numerical tests is that the solution at a vacuum boundary is sensitive to the mesh size Δx used in the calculation and also sensitive to how the boundary parameters are evaluated. To study this phenomenon, we consider a steady-state transport problem in a homogeneous slab with a constant (and unity) incident flux on the left boundary and a vacuum boundary on the right. Further we assume isotropic scattering with the scattering ratio $c = \sigma_s / \sigma = 0.3$. With the spatial variable x given in MFP, the transport equation for this problem is

$$\mu \frac{d\psi}{dx} + \psi = \frac{c}{2}\phi . \tag{28}$$

Then its flux-limited diffusion approximation is

$$-\frac{d}{dx}(D\frac{d\phi}{dx}) + (1-c)\phi = 0 \tag{29}$$

with the boundary conditions given in the form of

$$F_{inc} = \frac{1}{2}[\beta\phi \mp D\frac{d\phi}{dx}] \quad (30)$$

where the signs – and + are for the left and right boundaries, respectively. Specifically, we have $F_{\text{inc}} = ½$ at the left boundary and $F_{inc} = 0$ at the right boundary. The solutions of different methods for this problem are plotted in Fig. 4, which shows that the D_M solution is much better than P_1 and D_{LP}. However, the D_M solution (also the LP solution) at the vacuum boundary (x = 10) is found to be sensitive to the mesh sizes and the way that the parameters (D and β) in Eq. (30) are evaluated; while the solution at the incident boundary (x = 0) is not.

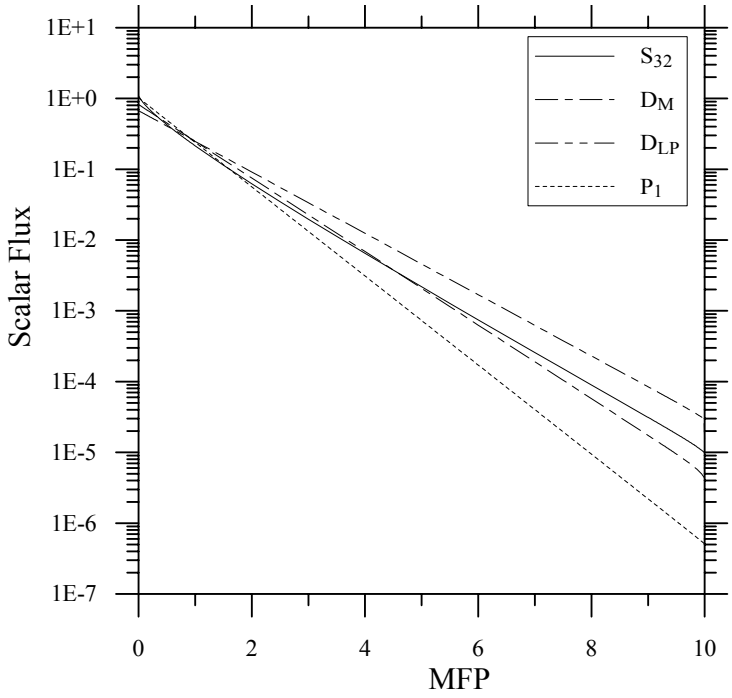

Figure 4. Solutions for a Deep Penetration Problem

Before showing these results, let's first look at several different ways to evaluate the parameters (D and β) for the boundary conditions. In the flux-limited diffusion calculations, ϕ is usually solved at cell centers and D is regarded as a constant within a cell, evaluated at cell center. After ϕ is obtained at cell centers after on iteration, ϕ at each cell edge is then computed as a weighted average of the fluxes at the two adjacent cell centers, according to the conservation of current. Then the parameter R is calculated at cell centers, which is subsequently used to calculate D at cell centers for the next iteration. Please see Ref. [13] for the detail of this procedure. Consistent with this practice, D in the boundary condition given by Eq. (30) is also taken as the value evaluated at the boundary cell center; so is β for convenience. That is, we use the following boundary condition (called treatment A)

$$F_{inc} = \frac{1}{2}\left[\beta_c\phi_b \mp D_c\left(\frac{d\phi}{dx}\right)_b\right], \quad (31)$$

where subscripts b and c denote boundary edge and boundary cell center, respectively. Using this treatment, we found that the converged flux ϕ (to the pointwise relative error of 10^{-6}) and β at the vacuum boundary change significantly with the mesh size Δx; however, the converged ϕ and β at the incident boundary don't. We then tried the second treatment (B) for the boundary conditions, in which the boundary parameter β is evaluated at the boundary (cell edge), i.e.,

$$F_{inc} = \frac{1}{2}\left[\beta_b\phi_b \mp D_c\left(\frac{d\phi}{dx}\right)_b\right]. \quad (32)$$

Once again, this treatment has the same problem as the first treatment, only the converged values for ϕ and β at the vacuum boundary are different from those obtained by the treatment A. Finally, we used the third treatment (C) in which both ϕ and β are evaluated at the boundary:

$$F_{inc} = \frac{1}{2}\left[\beta_b \phi_b \mp D_b \left(\frac{d\phi}{dx}\right)_b\right]. \tag{33}$$

This time, the converged values for ϕ and β at the vacuum boundary don't change with the mesh size Δx any more. The converged results at both boundaries for the three treatments are listed in Tables I and II. As shown, the solutions at the incident boundary are almost invariant to mesh sizes and the different ways of treating the parameters used in the boundary condition. But the solutions at the vacuum boundary are too sensitive to these variations. Similar behaviors are also observed for the LP flux–limited diffusion method.

Table I. Scalar Flux and Parameter β at the Incident Boundary x = 0.

Cell Size Δx	A: D_c β_c		B: D_c β_b		C: D_b β_b	
	β	ϕ	β	ϕ	β	ϕ
0.1	0.638972	0.817735	0.638579	0.817998	0.637921	0.818226
0.05	0.638748	0.817090	0.638650	0.817155	0.638464	0.817249
0.01	0.638676	0.816883	0.638672	0.816886	0.638664	0.816891
0.001	0.638673	0.816875	0.638673	0.816875	0.638673	0.816875

Table II. Scalar Flux and Parameter β at the Vacuum Boundary x = L.

Cell Size Δx	A: D_c β_c		B: D_c β_b		C: D_b β_b	
	β	ϕ	β	ϕ	β	ϕ
0.1	0.689497	4.57503E-6	0.698423	4.52625E-6	0.787318	3.96311E-6
0.05	0.706440	4.49778E-6	0.714198	4.45555E-6	0.787311	4.04813E-6
0.01	0.747284	4.28523E-6	0.751574	4.26323E-6	0.787307	4.08453E-6
0.001	0.779825	4.12253E-6	0.780767	4.11795E-6	0.787306	4.08636E-6

To find the reason of such strange behavior, we rewrite the boundary conditions in terms of β, λ and R. By the definition of D, we have

$$-D\frac{d\phi}{dx} = -\frac{\lambda(R)}{\sigma_{eff}}\frac{d\phi}{dx}. \tag{34}$$

According to

$$R = \frac{1}{\sigma_{eff}\phi}\left|\frac{\partial\phi}{\partial x}\right| \tag{35}$$

(R is always non-negative), Eq. (34) becomes

$$-D\frac{d\phi}{dx} = \lambda(R)R\phi, \tag{36}$$

since $d\phi/dx$ is negative in this problem. Substituting this result in Eq. (30) and dividing the both sides by ϕ, we obtain that at the left incident boundary where $F_{inc} \neq 0$, the boundary condition is

$$\beta(R) = \frac{2F_{inc}}{\phi} - \lambda(R)R . \qquad (37)$$

At the right boundary where $F_{inc} = 0$, the vacuum boundary condition becomes

$$\beta(R) = \lambda(R)R . \qquad (38)$$

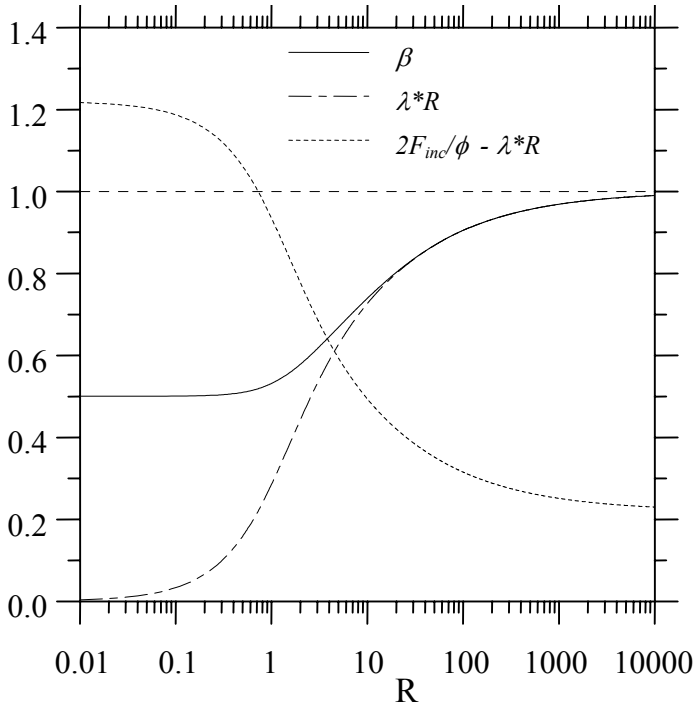

Figure 5. Parameters for the Boundary Conditions

The curves of $\beta(R)$, $\lambda(R)R$ and $\left[2F_{inc}/\phi - \lambda(R)R\right]$ are plotted as the functions of R in Figure 5. Clearly, there is a crossing point between the curves β and $\left[2F_{inc}/\phi - \lambda(R)R\right]$. Thus, for a given non-zero F_{inc}, there always exists a non-zero R (which is a function of ϕ) that satisfies the incident boundary condition given by Eq. (30) or (37). This explains why the converged value for R (also for β and ϕ) at the incident boundary is insensitive to mesh size and the ways of treating the parameters in the boundary condition, because such variations only cause very small changes in the quantities involved in the equation.

However, for the vacuum boundary condition, the curves β and λR in fact don't cross each other; they only asymptotically approach to each other at large R. Theoretically, the vacuum boundary condition or Eq. (38) has no solution except at $R \to \infty$, which yields $\beta = 1$. This means that in theory the iteration for β should never converge. However, from a practical viewpoint, the difference between β and λR becomes negligibly small when R is large enough (say $R > 20$). So after a number of iterations, β is regarded as "converged" at some value. For the treatment C where all the variables are evaluated at the true boundary [i.e., $\beta(R_b) = \lambda(R_b)R_b$], iterating β is exactly trying to find a crossing point between the two curves of β and λR. Accordingly, mesh size almost has no effect on the iteration and the "converged" value of β, as shown in Tables I and II. In addition, one can imagine that a large number of iteration is required to reach the "converged" value for β, due to the asymptotic approaching between the two curves. The iteration numbers of the three different treatments for the boundary conditions to converge the scalar flux to different convergent criteria are listed in Table III, which confirms the above analysis.

For the other two treatments, the three variables in Eq. (38) are not evaluated at the same point: the treatment A in fact is iterating $\beta(R_c) = \lambda(R_c)R_b$ and the treatment B is iterating

$\beta(R_b) = \lambda(R_c)R_b$. Due to the difference between R_b and R_c, the iteration process in fact is trying to find a crossing point between the two "shifted" curves. Apparently, the crossing point depends on $\Delta R = R_b - R_c$, which depends on the mesh size Δx. Although ΔR is very small, it can cause noticeable difference for the converged value for β due to the asymptotic approaching nature between the two curves. Because of that, the converged values for β and ϕ obtained by these two treatments are sensitive to mesh size, as demonstrated in Tables I and II. In addition, by shifting the curves, it is much easier to reach a solution than the treatment A. This is also demonstrated in Table III.

Table III. Iteration Numbers for Different Treatments at $\Delta x = 0.1$.

Convergent Criterion	A: D_c β_c	B: D_c β_b	C: D_b β_b
10^{-3}	13	15	50
10^{-4}	26	30	146
10^{-5}	40	44	253
10^{-6}	53	59	362

Please note that the determination of the boundary parameter β at the vacuum boundary in fact doesn't affect the whole solution significantly. In Figure 6 are plotted the DM solutions for the problem by using fixed $\beta = 1/2$ (the lower limit), $\beta = 1$ (the upper limit), and the iterated β (by treatment A) at the vacuum boundary, respectively. As shown, β only slightly affects the solution near the vacuum boundary (where the flux-limited diffusion solution is not accurate anyway). Therefore, one can still use the DM method in transport calculations to estimate a solution, although the boundary condition given by Eq. (30) has the ambiguity problem at a vacuum boundary as just discussed. For an incident boundary, it doesn't matter how to evaluate the parameters β and D in the boundary condition, because all the treatments practically produce the same results. For convenience, however, one may want to evaluate β and D used in the boundary condition at the center of the boundary cell (treatment A), due to its convenience. For a vacuum boundary, we suggest to either evaluate β and D in the

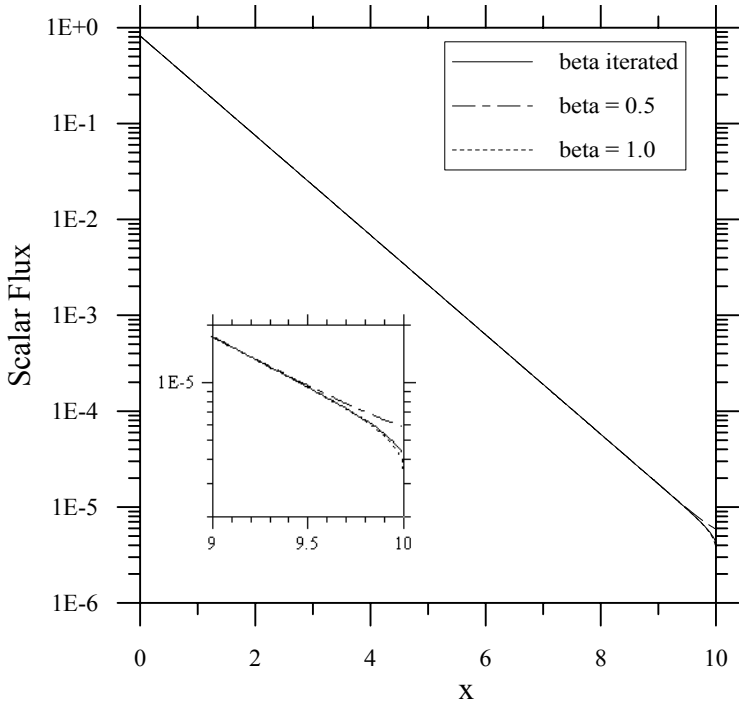

Figure 6. Impact of Beta on the DM Solution

boundary condition at the center of the boundary cell, due to its convenience and relatively faster convergence (but one needs to remember that this treatment makes the solution at the vacuum boundary sensitive to mesh size) or simply use a pre-fixed large R solution (such as $\beta \approx 0.8$ evaluated at $R = 20$) in the vacuum boundary condition.

5. CONCLUDING REMARKS

The DM flux-limited diffusion method uses a nonlinear diffusion coefficient, which depends not only upon material property but also upon the flux and its spatial derivative. Due to this, the method captures more transport effects than the classic diffusion so it can perform reasonably well for those problems that the classic diffusion doesn't work for. However, some trade-off has to be paid. Although predicting quantitatively better solutions, using a nonlinear diffusion coefficient may cause some unphysical behaviors. One of such behaviors is that this method, just like the Minerbo Eddington factor method, predicts physically wrong changing pattern of attenuation coefficient with the scattering ratio in some range for steady-state, homogeneous, deep penetration problems. This phenomenon was discussed earlier [7,8]. This paper presents another unphysical behavior: the radiation energy near an incident boundary may decrease with time at very early times for time-dependent, incidence-driven, wave penetration problems, if very small temporal and spatial mesh sizes are used. This behavior and its cause are discussed in Sec. 3.

Others discussed in this paper are for the strange behavior of a boundary condition at a vacuum boundary. The boundary condition given in the paper for the DM equation yields some ambiguity in the solution at a vacuum boundary. Naturally, one would like to develop a better vacuum boundary condition that could yield a unique solution, just like the incident boundary condition. However, there may be a logical difficult for this. The Minerbo Eddington factor method and the DM flux-limited diffusion are based on the assumption that the angular flux (in one dimension) follows the form $\psi(x,\mu) \propto \exp[b(x)\mu]$, with b undetermined. When there is an incident flux at the boundary, one can use that information somehow, such as to conserve the partial current at the boundary, to determine the unknown constant b. Once b is known, a boundary condition can be developed. However, at a vacuum boundary, no information is available to determine b. Hence, specification of a good vacuum boundary condition is quite challenge. The boundary condition given in the paper was developed at an incident boundary but is forced to use at a vacuum boundary with $F_{inc} = 0$. The boundary condition for the L-P flux-limited diffusion given in [13] was developed in the same way (but with a different assumption for angular dependence) and thus it demonstrates the same behavior at a vacuum boundary as DM; the reason is also the same as discussed in Sec. 4 for the DM flux-limited diffusion method.

REFERENCES

1. G.N. Minerbo, "Maximum entropy Eddington factors," *J. Quant. Spectrosc. Radiat. Transfer* **20**, pp. 541-545 (1978).
2. C.D. Levermore and G.C. Pomraning, "A flux-limited diffusion theory," *Astrophys. J.* **248**, pp. 321-334 (1981).

3. C.D. Levermore, "Relating Eddington factors to flux limiters," *J. Quant. Spectrosc. Radiat. Transfer* **31**, pp. 149-160 (1984).
4. H. Janka, "Flux-limited neutrino diffusion versus Monte Carlo neutrino transport," *Astron. Astrophys.* **256**, pp. 452-458 (1992).
5. B.J. Su, "Variable Eddington factors and flux-limiters for radiative transfer," *Nuclear Science & Engineering* **137**, pp. 281-297 (2001).
6. A. Korner and H. Janka, H., "Approximate radiative transfer by two-moment closure – when is it possible?" *Astron. Astrophys.* **266**, pp. 613-618 (1992).
7. T.A. Brunner, J.P. Holloway, J.P., and E.M. Larsen, E.M., "On the use of maximum entropy Eddington factors in shielding calculations," *Trans. Am. Nucl. Soc*. **77**, pp. 195-196 (1997).
8. B.J. Su, M.G. Fried, and E.W. Larsen, "Stability analysis of the variable Eddington factor method," *Transp. Theory Stat. Phys*. **30**, pp. 439-455 (2001).
9. T.A. Brunner and J.P. Holloway, "Using an approximate Riemann solver with the maximum entropy closure," *Trans. Am. Nucl. Soc.* **79**, pp.128-129 (1998).
10. T.A. Brunner and J.P. Holloway, "One-Dimensional Riemann Solvers and the Maximum Entropy Closure," *J. Quant. Spectrosc. Radiat.* **69**, pp. 543-566 (2001).
11. C.K. Yin and B.J. Su, "A nonlinear diffusion theory for particle transport in strong absorbers," *Annals of Nuclear Energy*, **29**, pp. 1403-1419 (2002).
12. C.K. Yin and B.J. Su, B.J., "A flux-limited diffusion theory derived from the maximum entropy Eddington factor," *Trans. Am. Nucl. Soc.* **84**, pp. 228-229 (2001).
13. R.H. Szilard and G.C. Pomraning, "Numerical Transport and Diffusion Methods in Radiative Transfer," *Nuclear Science and Engineering* **112**, pp. 256-269 (1992).